

Tunable Diode Laser Diagnostics of Halon Replacement Agents and Other Combustion Species

Robert G. Daniel, Kevin L. McNesby, and Andrzej W. Miziolek

U.S. Army Research Laboratory
AMSRL - WT - PC
Aberdeen Proving Ground, Maryland 21005-5066

1. ABSTRACT

Tunable diode laser absorption spectroscopy (TDLAS) is proving to be a valuable tool for species monitoring in Halon replacement combustion research. TDLAS is being used to characterize low pressure, premixed methane/oxygen/argon flat flames inhibited with prospective Halon replacement agents and Halon 1301 (CF₃Br). Species concentration profiles are measured spectroscopically by either direct absorption or derivative spectroscopy. Species temperature profiles are measured spectroscopically using the method of Two-Line Thermometry, and flame temperature is measured with fine wire thermocouples. The advantages of the diode laser technique, as well as results of recent studies, are discussed.

2. INTRODUCTION

Infrared absorption spectroscopy has been used to characterize low-pressure, premixed methane/oxygen flat flames inhibited by candidate Halon alternative compounds. The infrared radiation (IR) source for this study is a tunable diode laser, which, due to its narrow linewidth (0.0005 cm⁻¹), allows the observation of individual ro-vibrational transitions for many flame species using the technique called Tunable Diode Laser Absorption Spectroscopy (TDLAS). The flames are characterized by measuring temperature and species profiles as a function of height above the burner surface.

Through the course of this study, and as has been demonstrated in many previous studies, tunable diode laser spectroscopy has proven to be an effective and versatile technique for monitoring combustion environments. Many flame species, both major and minor, have been observed by taking advantage of the narrow linewidth of the diode laser (see Table 1). Due to the number of observable species, this technique is proving to be nearly comparable to the molecular beam/mass spectrometer (MB/MS) flame diagnostic technique with respect to the number of species detected. The advantages of the present system over an MB/MS system are the cost of operation, the size and amount of equipment, and the ability to locate the equipment in any real-world combustion environment where line-of-sight measurements are accessible. Although these two techniques (MB/MS and TDLAS) are somewhat complementary in performance, the TDLAS system has a major advantage as it is non-intrusive. TDLAS can also be compared to Laser Induced Fluorescence (LIF), with both techniques having relative strengths and weaknesses. TDLAS can more readily produce quantitative species concentrations than can LIF and can detect polyatomic species that do not fluoresce.

The results of this experimental study are being used to validate a chemical kinetic mechanism being developed at the National Institute of Standards and Technology [1], that

describes the chemistry of fluorine-containing compounds in combustion environments. The development of this database has been expanded to include bromine chemistry, and current work is addressing iodine chemistry as well [2]. Our specific interest is the flame inhibition mechanisms of fluorine-containing compounds which are being considered as possible replacements to the presently used fire extinguishing agents Halon 1301 (CF_3Br) and Halon 1211 (CF_2ClBr). In accordance with the Montreal Protocol and its amendments [3], as of January 1, 1994, the manufacture and sale of these compounds are prohibited, except for those which have been recycled. The possible replacement compounds of current interest are hydrochlorofluorocarbons (HCFCs), hydrofluorocarbons (HFCs), perfluorocarbons (PFCs), and fluoroiodocarbons (IFCs). The HCFCs are an interim solution as they are scheduled to be phased out, so have not been included in this study.

3. EXPERIMENTAL

The apparatus can be divided into three subsystems: gas handling, low-pressure burner, and radiation source and detection systems. The gas handling system consists of flow controllers for each of the principal gases introduced to the low-pressure burner chamber. An MKS 147B mass flow controller is used to control MKS model 2159B flow meters to introduce the fuel (CH_4), oxidizer (O_2), diluent (Ar), and shroud (Ar) gases. The stated accuracy is $\pm 1\%$ of the full scale of the flow valve, so the maximum deviation will be 0.1 L/min, and the repeatability is quoted as $\pm 0.2\%$ of the reading. Inhibitant gases are introduced through either a Matheson model 601 gas rotameter which has been calibrated with a wet test meter (CGA/Precision Scientific) or an MKS gas flow meter. The fuel, oxidizer, and argon gases were Matheson UHP grade and used without further purification. The inhibitant gases, of varying purity, were obtained from either Matheson or PCR and used with no further purification.

The low-pressure burner assembly consists of a flat flame burner (McKenna Industries, Inc.) mounted in a cylindrical vacuum chamber (Huntington Vacuum). The flat flame burner is composed of concentric stainless steel frits through which the combustion and shroud gases flow. The combustion gases enter a mixing chamber immediately beneath the 6 cm diameter center frit. The gases flow through the frit, and the flame front is stabilized by this surface. The height of the flame above the burner surface is dependent on the flame velocity. Shroud gas flows through a fritted 1 cm wide annulus surrounding the center frit. The shroud gas helps to stabilize the flame and helps to maintain laminar flow of the premixed combustion gases. The burner head temperature (typically 50 - 90 °C) is monitored by a thermocouple cemented to the burner head near the outer (shroud gas) annulus. The burner head is mounted on both horizontal and vertical translation stages which provide a full range of motion for flame diagnostics.

The cylindrical vacuum chamber has four optical ports separated by right angles located 10 in. above the chamber base. Two of these ports define the line-of-sight of the laser for the experiment, and the burner head is translated relative to this fixed axis. The windows in the line-of-sight of the laser are either NaCl or CaCl_2 , depending on the frequency region being studied. One optical port perpendicular to the laser beam path is a 4 in. hinged view port, which serves as an access port to light the flame. The remaining port has a linear motion feedthrough on which is mounted a fine wire thermocouple. This feedthrough allows the thermocouple to be withdrawn completely from the flame during optical monitoring.

Exhaust gases are removed through the top of the low-pressure chamber by a Leybold SV-100 high-volume vacuum pump. The gases are removed through the top of the chamber to help

maintain the laminar flow of the gases through the burner chamber. Coarse control over the chamber pressure is accomplished by the use of an MKS model 253A butterfly valve. Fine control of the pressure is obtained by a precision needle valve (open to atmosphere) that is located just prior to the butterfly valve. This valve combination allows the pressure to be set and maintained to within several millitorr throughout the duration of an experiment. The pressure of the chamber is measured at the base of the chamber, below the burner head, by an MKS model 390HA capacitance manometer with a 100 torr range.

The tunable diode laser system (Laser Photonics, Analytics Division, Inc.) consists of a cryogenically cooled Pb salt laser source, a monochromator for mode selection, and IR detectors. The diode lasers are cooled using either a liquid nitrogen cooled dewar or an He refrigerator depending on the spectral range being investigated. The multimode output of the diode is collected by a parabolic mirror and passed through the grating monochromator. The monochromator acts as a mode filter and provides coarse ($\sim 2 \text{ cm}^{-1}$) frequency identification. A mechanical chopper provides for lock-in detection. The monochromator has a resolution of 0.5 cm^{-1} , which allows the selection of individual modes of the diode as these modes are separated by greater than 1 cm^{-1} . The IR beam then passes through two beam splitters before passing through the low-pressure burner assembly. One of the split beams passes through a passive confocal etalon which, when scanning the frequency, produces interferometer fringes for precise frequency calibration. The second split beam passes through one or two gas reference cells which are used to identify and calibrate the absolute frequency of the laser. Both beams are detected by LN₂-cooled HgCdTe detectors. A parabolic mirror focuses the radiation through the burner assembly, and a hyperbolic mirror collects and focuses the radiation on an LN₂-cooled HgCdTe detector. The beam diameter of the IR radiation at the burner head is typically 0.75 mm.

Data collection occurs by one of two methods. The first employs phase sensitive-detection. The output of the IR detectors is passed to lock-in amplifiers which use the frequency of the chopper as a reference. This frequency is supplied as a TTL pulse from the monochromator. The AC output of the lock-in amplifiers is passed to an A/D converter interfaced to a personal computer. The personal computer also controls the current sweep of the diode laser. Data collection is managed by a program supplied by Laser Photonics. This program, while useful, necessitates long collection times (40 s/scan) for single data sets. Typically eight scans are co-added and averaged at each burner position to compose a data set, after which the data is transferred to a second personal computer for handling and final analysis.

The second approach uses a recently acquired LeCroy 9360 digital oscilloscope, which has a much faster data acquisition rate than the previous method, collecting and averaging the direct output of the IR detectors. This allows an increase in the number of co-added scans from 8 to 500, which leads to an increase in the signal-to-noise ratio. The files collected by the digital scope are transformed into ASCII files before being passed to a personal computer for analysis.

Since the data are collected as single beam spectra, a background spectrum is collected for each data set with the flame off and no gas flow. The observed spectra are ratioed to this background spectrum. This ratio accounts for the variation in diode laser intensity as a function of tuning current. This normalization procedure also accounts for output power differences of the diode between data sets. It was observed that power variations, caused by minor adjustments of the diode laser between subsequent runs, resulted in significant differences between data sets.

Flame temperatures are also measured using Pt/10%Pt-Rh fine wire ($100 \mu\text{m}$) thermocouples which have been coated with a refractory mixture of yttrium oxide and beryllium

oxide [4]. The high emissivity of this ceramic sheath reduces the internal temperature of the thermocouple junction, as the flame temperature may exceed the melting point of platinum. The sheath also minimizes errors caused by platinum-catalyzed reactions at the thermocouple junction.

4. DATA ANALYSIS

The collected spectra are analyzed in one of two ways depending on the identity of the absorbing species. Carbon monoxide spectra are analyzed to measure the concentration profile and also to measure the temperature of the flame. The spectrum is fit to a mathematical model of the transmission, and both concentration and temperature are extracted. The spectra of the other flame species are analyzed for concentration only, relying on the temperature from the thermocouple or that determined by the CO spectra for the calculations. The available literature spectra of each molecule is used to extract the concentration profiles, either relative concentration between different flames or absolute concentration when possible. Both of these methods are outlined below.

a. Carbon Monoxide (CO)

The method of two-line thermometry [5] is used to determine from spectra the temperature and CO concentration profile of the flame under study. The temperature and the concentration of CO are extracted from the measurement of two closely lying ro-vibrational transitions of CO originating from excited vibrational states. The flame temperature and CO concentration are extracted from the ratio of the integrated absorbance of the two transitions.

The experimental transmission spectrum can be mathematically described by the Bouguer-Lambert law of absorption [5] as:

$$\tau(\nu) = \left(\frac{I}{I_0} \right) = \exp \left(- \left[S_{w,j} \phi(\nu-\nu_0) L P_x \right] \right) \quad (1)$$

where $S_{w,j}(T)$ is the line strength of the transition, $\phi(\nu-\nu_0)$ is the line shape function, L is the path length of the absorbing species (nominally set by the dimension of the burner head), and P_x is the partial pressure of absorbing species x . The normalized single beam spectrum is fit to the expression:

$$\tau(\nu) = \sum \exp \left(- \left[\alpha_i(T) V_i(\alpha, \chi) \right] \right) + A \quad (2)$$

with the summation being each ro-vibrational transitions measured in the spectrum. Here $\alpha_i(T)$ is the product of the line strength of the i^{th} transition and the pressure of the absorbing species, and $V_i(\alpha, \chi)$ is the Voigt function, calculated about the line center $\chi = (\nu-\nu_0)/\Delta\nu_D$, where $\Delta\nu_D$ is the Doppler width. The fitting function includes a cubic baseline (A) to account for the nonlinear output of the diode laser.

The observed CO spectrum is fit to the above equations using a nonlinear least squares fitting routine [6]. The Voigt profile is calculated using a summation approximation to the complex error probability function [7]. The output of this program contains, for each transition, an α_i , a broadening parameter, a frequency shift, and the baseline parameters. The temperature of the species being measured is calculated from the ratio of the observed α_i with values of the ratio of the calculated line strengths:

$$F(T) = \frac{S_{\omega}^H(T)}{S_{\omega}^I(T)} = \frac{\alpha^H(T)}{\alpha^I(T)}. \quad (3)$$

The pressure of the absorbing species is obtained from the definition of the α ; once the temperature has been calculated:

$$P_x = \frac{\alpha^I(T)}{S_{\omega}^I(T)}. \quad (4)$$

The line strengths of the individual ro-vibrational transitions are calculated from an expression referencing the literature value of the fundamental band strength of the transition [5]. These calculated line strength values are used to construct the $F(T)$ found in Equation (3). The expression to calculate the line strength for a transition at a temperature T is:

$$S_{\omega}(T) = S^1(T_0) \frac{T_0}{T} \frac{\nu}{\bar{\nu}(T_0)} \frac{1}{Q(T)} (v+1) J \exp[-E''hc/k_B T] \times (1 - \exp(-hcv/k_B T)) (1 + x_e v) \quad (5)$$

where $S^1(T)$ is the fundamental band strength at reference temperature T_0 ; E'' is the energy of the initial state from which the transition originates, computed by:

$$E''(v, J) = \sum_{i,k} Y_{i,k} \left(v + \frac{1}{2} \right)^i [J(J+1)]^k \quad (6)$$

where Y_{ik} are the Dunham coefficients in wavenumbers [8]; $(1 + x_e v)$ is a mechanical anharmonicity factor which is included for vibrationally excited initial states; $Q(T)$ is the partition function at temperature T calculated by:

$$Q(T) = \sum_{v,J} (2J+1) \exp[-E''(v, J)hc/k_B T]; \quad (7)$$

$(1 - \exp(-hcv/k_B T))$ is a correction factor for induced emission from excited states necessary for elevated temperatures; and $\bar{\nu}(T_0)$ is the effective band center. The goodness of the fit is measured by the Chi Squared test. Data sets for each flame and position within the flame are collected four times, and the results of these four sets examined for inconsistencies before being averaged to produce the final value of temperature and concentration used as characteristic of the flame.

In a previous study [9], the final values of spectroscopically measured flame temperatures were found to be consistently lower than the values measured by fine wire thermocouples. In this study, the distribution of CO across the burner head was measured using tomographic analysis [9]. The flame temperatures obtained from the spectroscopic measurements are corrected to account for absorption by CO lying outside of the burner region. The reduced absorbance of the individual transitions translates to a higher temperature than originally calculated and is illustrated in Figure (1), in which both thermocouple and spectroscopic temperatures (both corrected and uncorrected) are included.

Figure (2) presents the CO concentration and temperature profiles, analyzed using two-line thermometry, of methane/oxygen flames inhibited with 1.0% of the fluoromethanes. It is readily seen from the figure that each agent produces unique behavior in the flame.

b. Other Species

The concentration profiles of the other species observed using IR absorption spectroscopy and employing the LeCroy 9360 digital oscilloscope are analyzed by either of two methods. The first method obtains relative concentrations of the species for comparison between flames inhibited with different agents by integrating the normalized absorbance of a specific transition of the molecule being studied and comparing the relative intensities between the different flames. Figure (3) shows the relative concentration of CH, disappearance and H₂O appearance for both an uninhibited flame and a flame doped with 1% CF₃H. The vertical dashed lines represent the position of the flame front. The visible change in position is due to a change in the flame velocity and to the fact that the total pressure of that flame is 20 torr. When the pressure is raised to 32 torr, the change in the flame position upon agent addition is reduced, and is not seen either in the species profiles or by visible observation.

The second method, under development, determines the absolute concentration of the species of interest by using the line strength of the transition of interest. The transition is first identified by comparison with exact line positions from the literature. The temperature of the species is calculated by one of the two methods described previously. The temperature dependence of the individual transitions are taken into account by relying on previous spectroscopic work available in the literature. This information is then used to extract an absolute concentration of the species. The molecules presently under study are CH, H₂O, and CF₂O.

Even without absolute concentrations for all species observed, the information obtained has proven useful for the validation of the chemical kinetic mechanism describing fluorine chemistry in flames. Figure (4)a shows the calculated disappearance profiles of three fluoromethane agents in a 20 torr, freely propagating methane/air flame, and (4)b shows the observed relative disappearance profiles of the same agents in a 20 torr burner stabilized methane/oxygen flame. Qualitative agreement is easily with the present modeling results. Work is continuing on the modeling to incorporate the experimental conditions to allow for direct comparison with the experimental results.

Figure (5) presents recent results of the appearance profile of CF₂O in flames inhibited with the candidate Halon replacement compounds FE-13 (CF₃H) and HFC-125 (C₂F₅H), and Halon 1301. The profiles show that more CF₂O, a toxic byproduct of the combustion process, is produced by both alternative agents than by Halon 1301. Other qualitative differences in the activity of these agents is illustrated in the next four figures which show an uninhibited flame and flames inhibited with 1.0% of the three agents. The most obvious change is the intensity of the two water transitions in this **spectral** region (1259.2 cm⁻¹). The intensity of the methane transition also increases upon the addition of all three agents due to a change in the species temperature within the flame resulting in a change in the population distribution of the molecular energy levels. Also shown are the different amounts of CF₂O produced.

5. CONCLUSIONS

We have observed 11 flame species present in premixed methane/oxygen flames inhibited by candidate Halon alternative agents using TDLAS. Both qualitative and quantitative concentration profiles of flame species and flame temperature profiles have been obtained. The data are being used in the validation of a chemical kinetic mechanism that describes halogenated flames. This study has shown the utility and versatility of TDLAS in the characterization of combustion systems.

This project is continuing in three directions. The first is the inclusion of more flame species. The detection of radical species is well within the capabilities of the present detection system, and the search for $\text{CF}_2\cdot$ and $\text{CF}_3\cdot$ is presently underway. Second, the project is undertaking the inclusion of atmospheric pressure diffusion flames, which more closely mimic real-world fire scenarios. This aspect has already started with a spectroscopic study of inhibited diffusion flames using an Fourier transform infrared spectrometer [10]. An opposed flow diffusion burner is presently under construction at the U.S. Army Research Laboratory. This study will include the theoretical modeling of inhibited diffusion flames [11]. The third aspect of the present project is the incorporation of a room temperature near-IR laser system for the detection of acid gases in flames. The acid gases (HF, HCl, HBr) do not have vibrational transitions in regions accessible to the cryogenically cooled lead salt diode lasers. The use of near-IR lasers for acid gas detection has shown promise for monitoring combustion processes and the combustion byproducts of halogenated flames [12].

6. ACKNOWLEDGMENTS

We would like to acknowledge funding for this project from the Strategic Environmental Research and Development Program (SERDP).

7. REFERENCES

1. P.R. Westmoreland, D.R.F. Burgess, Jr., W. Tsang, and M.R. Zachariah, *Proc. of the 25th Symp. (Int) on Comb.*, The Combustion Institute, Pittsburgh, PA, 1994.
2. V. Babushok and W. Tsang, National Institute of Science and Technology, private communication, 1994.
3. Copenhagen revisions to The Montreal Protocol on Substances That Deplete the Ozone Layer, 1992.
4. J.H. Kent, *Combustion and Flame*, **14** p279 (1970).
5. P.L. Varghese and R. K Hanson, *J. Quant. Spectrosc. Radiat. Transfer*, **24** p479 (1980).
6. P.R. Bevington, "Data Reduction and Error Analysis for the Physical Sciences", McGraw-Hill, New York, 1969.
7. J. Humlíček, *J. Quant. Spectrosc. Radiat. Transfer*, **21** p309 (1929).
8. T.R. Todd, C.M. Clayton, W.B. Telfair, T.K. McCubbin, Jr., and J. Plíva, *J. Mol. Spectrosc.*, **62** p201 (1976).
9. K.L. McNesby, R.G. Daniel, J.B. Moms, and A.W. Miziolek, *App. Optics* (in press).
10. K.L. McNesby, R.G. Daniel, J.M. Widder, and A.W. Miziolek, ARL Tech Report (in press).

11. M. Smooke, Yale University, private communication, 1994.

12. D.S. Bomse, D.C. Houde, D.B. Oh, J.A. Silver, and A.C. Stanton, "Optically Based Methods for Process Analysis", SPIE vol 1681, p138 (1992). D.S. Bomse, Southwest Sciences, Inc., private communication, 1994.

Table 1. List of the flame species observed in inhibited flames, the frequency region in which the molecule is observed in this study, and the molecular transition excited (where appropriate).

Species	Frequency (cm ⁻¹)	Transition
CO	2020 - 2100	
CO ₂	2020 - 2100	ν_3
CH ₄	1240 - 1280	ν_2 and ν_4 dyad
H ₂ O	1260 - 1275	ν_2
CF ₄	1250 - 1280	ν_3 and $2\nu_4$
CF ₃ H	1075 - 1100	ν_2
CF ₂ H ₂	1075 - 1120	ν_3
CF ₃ Br	1075 - 1120	ν_1 and $\nu_2 + \nu_3$
CF ₃ I	1075 - 1100	ν_1
C ₂ F ₅ H	1190 - 1250 1070 - 1170	? ?
CF ₂ O	1250 - 1275 1910 - 1970	ν_4 ν_1
NO	1910 - 1950	

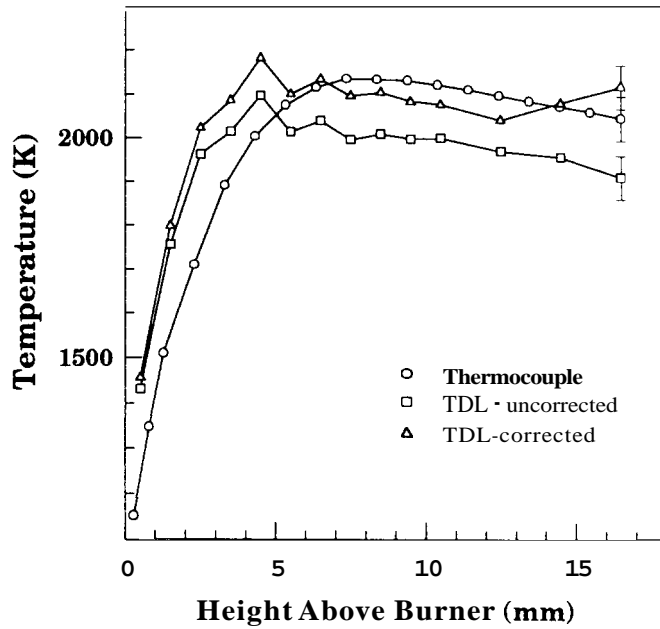


Figure 1. Flame temperature profiles of an uninhibited methane/oxygen flame measured spectroscopically and with a fine wire thermocouple.

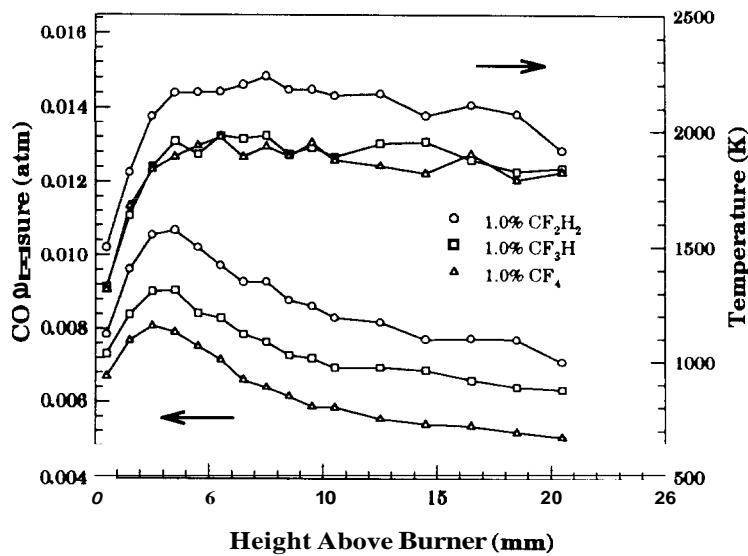


Figure 2. CO concentration and flame temperature profiles of 20 torr, stoichiometric, premixed methane/oxygen flames inhibited with 1.0% of the fluoromethanes. The observed trend in CO concentration is in qualitative agreement with calculations on freely propagating flames.

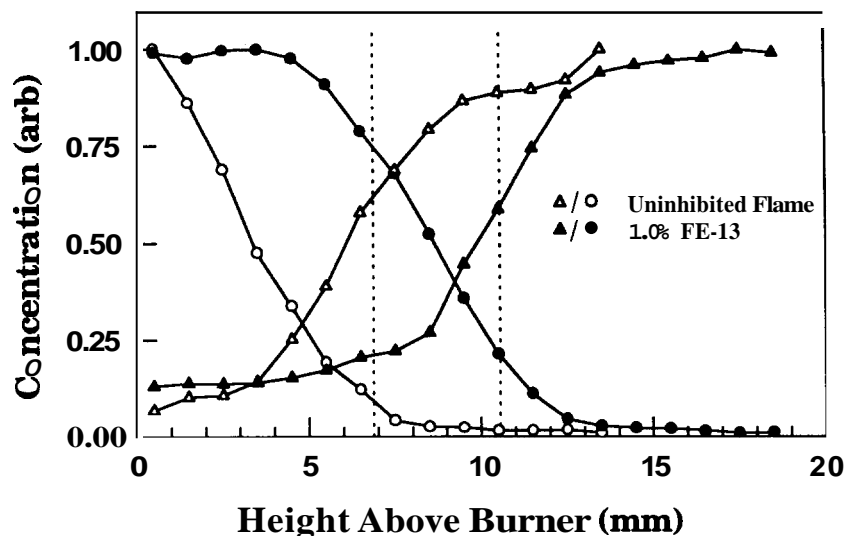


Figure 3. Methane disappearance profiles (circles) and water appearance profiles (triangles) for methane/oxygen flames. The vertical dashed lines mark the position of the flame fronts (inhibited flame furthest from the burner surface).

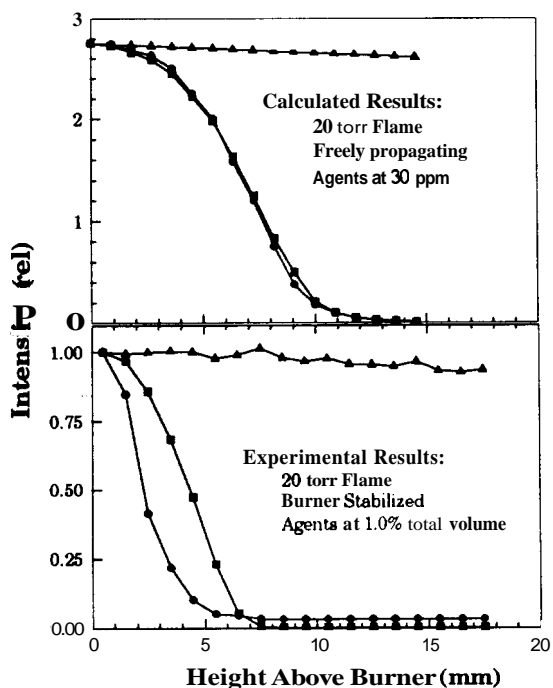


Figure 4. a) Theoretical disappearance profiles of the fluoromethanes in a freely propagating, 20 torr, methane/oxygen flame. All three agents were present at the 30 ppm level and the flame front is positioned at 0. We expect similar results for agents present at the 1.0% level. b) Experimental disappearance profiles of the fluoromethanes in a burner stabilized, 20 torr, methane/oxygen flame. The agents were present at 1.0% of the total flow by volume. (▲ - CF₄, ■ - CF₃H, and ● - CF₂H₂)

CF₂O Appearance for Inhibited Flames

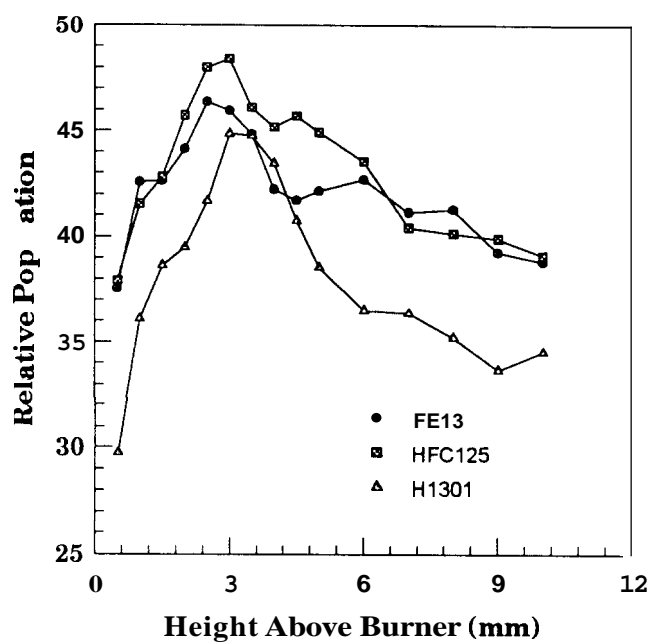


Figure 5. Appearance profiles of CF₂O for stoichiometric, 32 torr methane/oxygen flames inhibited with 1.0% of FE13 (CF₃H (circles)), HFC-125 (C₂F₅H (squares)), and Halon 1301 (CF₃Br (triangles)) as a function of height above the burner surface.

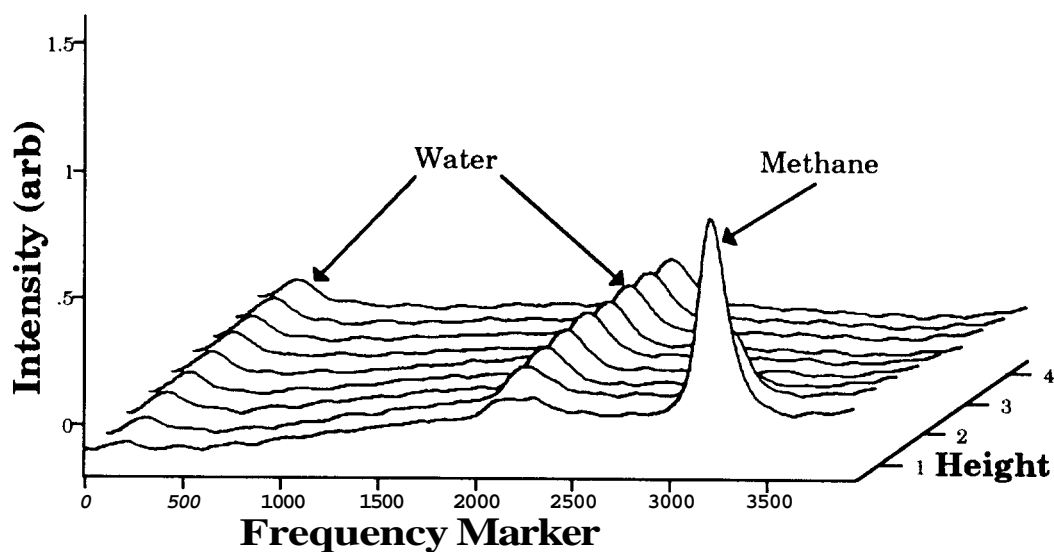


Figure 6. Three dimensional spectral profile of a methane/oxygen flame at 1259.2 cm⁻¹ as a function of height above the burner surface in millimeters. The total spectrum shown spans 0.22 cm⁻¹.

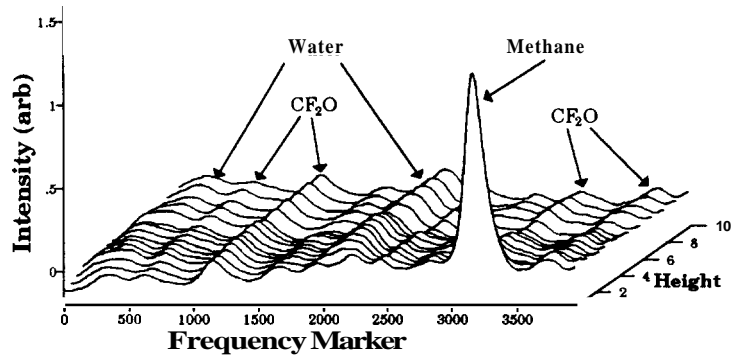


Figure 7. Three dimensional spectral profile of a methane/oxygen flame inhibited with 1.0% HFC-125 at 1259.2cm^{-1} as a function of height above the burner in millimeters. The total spectrum shown spans 0.22cm^{-1} .

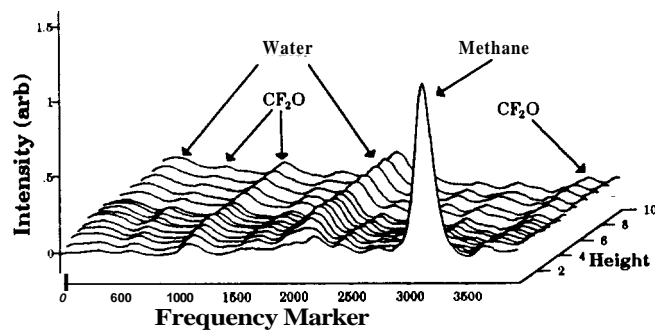


Figure 8. Three dimensional spectral profile of a methane/oxygen flame inhibited with 1.0% FE-13 at 1259.2cm^{-1} as a function of height above the burner in millimeters. The total spectrum shown spans 0.22cm^{-1} .

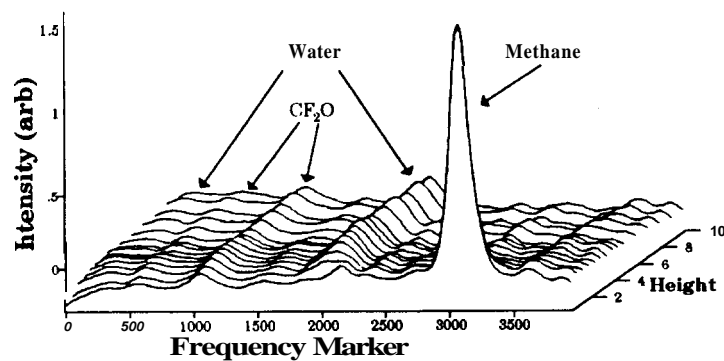


Figure 9. Three dimensional spectral profile of a methane/oxygen flame inhibited with 1.0% CF_3Br at 1259.2cm^{-1} as a function of height above the burner surface. The total spectrum show scans 0.22cm^{-1} .